JOURNAL OF GEOPHYSICAL RESEARCH, VOL. 87, NO. C13, PAGES 11,126–11,132, DECEMBER 20, 1982

A Stratospheric Chemical Instability

J. L. Fox[1], S. C. Wofsy, M. B. McElroy, and M. J. Prather

Center for Earth and Planetary Physics, Harvard University, Cambridge, Massachusetts 02138

The equations which determine partitioning of Cl_x in steady state have multiple (three) solutions under conditions which might arise in the high-latitude winter stratosphere. Two of these solutions are stable, one is unstable, to infinitesimal perturbations. The relative stability of solutions is examined by subjecting the system to finite perturbations. The more stable solution is found to eliminate the less stable when semi-infinite volumes of the two solutions are placed in contact. The high-ClO, low-NO_2 solution is more stable under most conditions. Transitions from less to more stable states are slow in winter but may occur more rapidly when the seasonal variation of insolation is taken into account.

Introduction

Chlorine compounds and oxides of nitrogen are found in concentrations of parts per billion or less in the terrestrial stratosphere. Considerable interest in the distribution and chemistry of these species has developed largely because they participate in catalytic chemical cycles which destroy stratospheric ozone (for a recent review see *World Meteorological Organization* [1981]). These cycles may be represented by

$$X + O_3 \rightarrow XO + O_2 \quad (1)$$

$$XO + O \rightarrow X + O_2 \quad (2)$$

where X is NO or Cl. The net result is destruction of odd oxygen:

$$O_3 + O \rightarrow 2O_2 \quad (3)$$

Chlorine compounds Cl_x are present in several inorganic forms including Cl, ClO, HCl, $ClNO_3$, and HOCl. The nitrogen oxide family, NO_y, includes NO, NO_2, $ClNO_3$, NO_3, N_2O_5, HNO_4, and HNO_3.

Prather et al. [1979] showed that the equations which describe partitioning of stratospheric Cl_x and NO_y admit multiple, physically reasonable solutions under certain conditions. They found that steady state concentrations of ClO and NO_2, as functions of the concentration of total inorganic chlorine, fall on S-shaped curves as shown in Figure 1*a*. There are three solutions to the steady state equations for a certain range of Cl_x, corresponding to species concentrations differing by up to several orders of magnitude. The steady state concentrations of other members of the Cl_x and NO_y families and of the HO_x family (OH + HO_2) exhibit similar behavior as shown in Figure 1*b*.

Our understanding of stratospheric chemistry has changed somewhat since the earlier study. Current models indicate that HNO_4 may play an important role in the lower stratosphere. Reaction of OH with HNO_3 is now thought to be rapid at low temperatures. It is clear that models for the chemistry of the lower stratosphere will continue to evolve. We elect here to retain the kinetic rates employed by *Prather et al.* [1979]. We demonstrate, however, that multiple solutions occur also with the more complete reaction schemes recommended by *NASA/JPL* [1981]. This paper is concerned with analysis of the stability of the three branches of solutions. Our emphasis is directed to the phenomenology of this problem, and our conclusions are unaffected by the details of the recent changes in kinetics. We conclude with a brief discussion of the implications of this work for present understanding of the stratosphere.

Origin of the Multiple Solutions

A qualitative understanding of the multiple steady states may be provided by a simple model with insolation averaged over 24 hours, with species and reactions as given in Table 1. The important reactions are shown schematically in Figure 2. Reactions (R1), (R2), and (R6) provide strong coupling between the NO_y and Cl_x families. The chemical lifetime of HNO_3 is long at high latitudes in winter, and HNO_3 is consequently decoupled from the rest of the NO_y family. We define NO_t to include all NO_y species except HNO_3. Interchange among members of the NO_t and Cl_x families occurs relatively rapidly. Concentrations of NO_t, HNO_3, Cl_x are specified consistent with observation.

At low concentrations of Cl_x, chlorine is present predominantly as HCl such that

$$[HCl] \approx [Cl_x] \quad (4)$$

The concentrations of chlorine radicals are given by

$$[Cl] = k_3[OH][HCl]/k_4[CH_4] \quad (5)$$

$$[ClO] = k_5[Cl][O_3]/k_6[NO] \quad (6)$$

and

$$[ClNO_3] = k_1[ClO][NO_2]/J_2 \quad (7)$$

Under these conditions the NO_t family (excluding $ClNO_3$) remains undisturbed by increases in Cl_x, and the concentration of OH, determined mainly by reactions involving NO_y,

$$OH + NO_2 \xrightarrow{M} HNO_3 \quad (R7)$$

$$OH + HNO_3 \rightarrow H_2O + NO_2 \quad (R28)$$

$$h\nu + HNO_3 \rightarrow OH + NO_2 \quad (R27)$$

is likewise unaffected by Cl_x.

Concentrations of Cl, ClO, and $ClNO_3$ increase linearly with Cl_x until, eventually, growth of $ClNO_3$ is limited by supply of NO_2. In this limit, large concentrations of Cl_x, $ClNO_3$ is the dominant NO_t constituent and

[1] Now at Center for Astrophysics, Harvard University, Cambridge, Massachusetts 02138.

Paper number 2C1434.
0148-0227/82/002C-1434$05.00

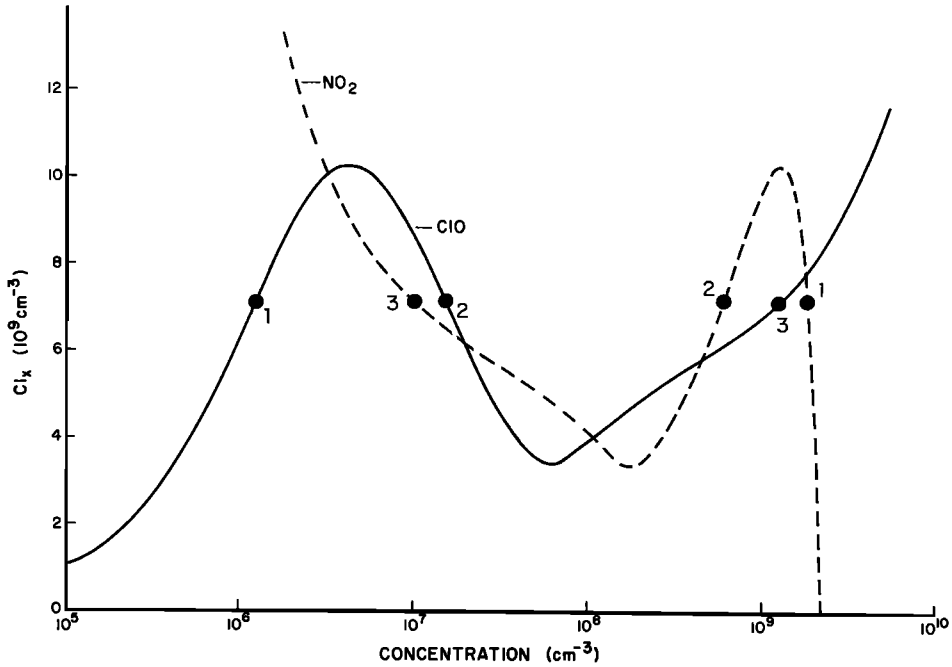

Fig. 1*a*

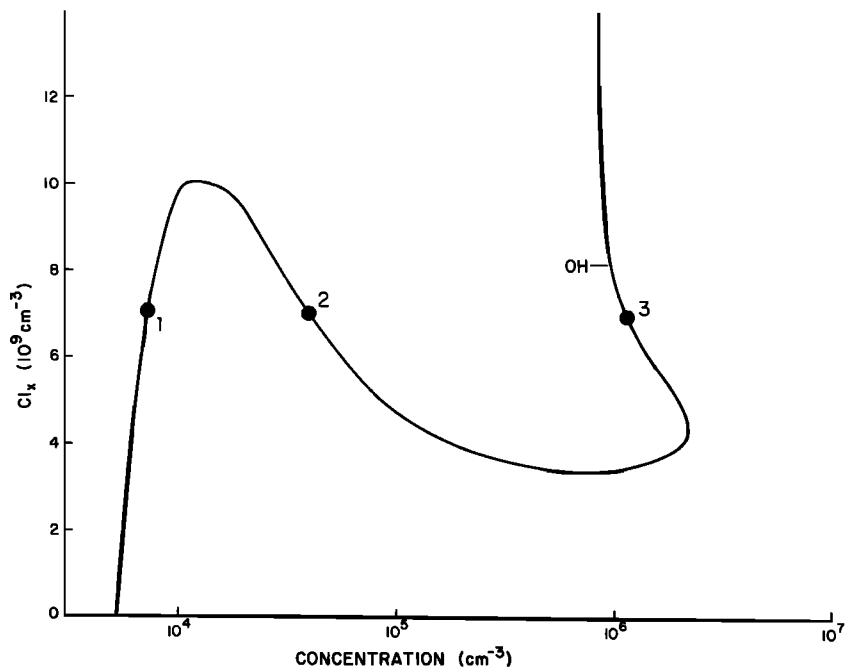

Fig. 1*b*

Fig. 1. Concentrations of ClO, NO_2 and OH plotted against the value of Cl_x which results from a steady state solution to the chemical model in Table 1. Three solutions exist for $3.5 \times 10^9 < Cl_x < 10 \times 10^9$ cm^{-3}. The points on each curve correspond to the solutions in Table 2.

$$[NO_2] = J_2[ClNO_3]/k_1[ClO] \ll [NO_t] \quad (8)$$

and

$$[NO] = J_9[NO_2]/\{k_8[O_3] + k_6[ClO]\} \propto [ClO]^{-2} \quad (9)$$

With further increase in ClO, NO_2 and NO are suppressed and return of Cl_x from ClO to HCl is inhibited. Consequently, ClO is the dominant component of chlorine at high Cl_x, NO and NO_2 are low, and $ClNO_3$ is the major form of NO_t. The concentration of OH increases as NO_2 decreases and reaction (R7) declines in importance. The concentration of ClO varies linearly with Cl_x in both high and low Cl_x limits, with a complex transition zone, the nature of which depends on OH. Location of the region of multiple solutions depends on the assumed kinetic model as well as on local conditions (e.g., temperature, pressure, sunlight). For the examples given here this region spans ClO densities from 10^6 to 10^9 cm^{-3}, corresponding to Cl_x mixing ratios of 0.3 to 6 ppbv. This range includes typical values observed in the contemporary stratosphere.

The concentration of ClO is approximately 0.1% that of Cl_x at low values of Cl_x. The transition zone corresponds to Cl_x approximately equal to $NO_t = 3 \times 10^9$ cm^{-3} for conditions in Figure 1. It may be shown that the loss rate for ClO in the transition zone decreases with increase in ClO. Net production of ClO is characterized by positive feedback and is consequently autocatalytic.

The occurrence of multiple steady states in autocatalytic reaction systems has been studied extensively in recent years [e.g., *Schlogl*, 1972; *Hahn et al.*, 1974; *Nitzan et al.*, 1974*c*; *Nicolis and Prigogine*, 1977]. The phenomenon was discussed initially for open systems with mass flow across boundaries [e.g., *Turing*, 1952; *Prigogine and Nicolis*, 1967; *Ortoleva and Ross*, 1971]. *Nitzan and Ross* [1973] and *Nitzan et al.* [1974*b*] showed that autocatalytic behavior can occur also for closed illuminated reaction systems.

TABLE 1. Photochemical Model for the Winter Stratosphere, 60°N at 12 km

Reaction/Constituent	Effective Rate Coefficients, cm^3 s^{-1} unless noted
(1) $ClO + NO_2 \rightarrow ClNO_3$	1.68×10^{-12}
(2) $ClNO_3 + h\nu \rightarrow ClO + NO_2$	6.54×10^{-6} s^{-1}
(3) $HCl + OH \rightarrow Cl + H_2O$	4.73×10^{-13}
(4) $Cl + CH_4 \rightarrow HCl + CH_3$	1.88×10^{-14}
(5) $Cl + O_3 \rightarrow ClO + O_2$	8.3×10^{-12}
(6) $ClO + NO \rightarrow Cl + NO_2$	1.7×10^{-11}
(7) $OH + NO_2 \rightarrow HNO_3$	9.38×10^{-13}
(8) $NO + O_3 \rightarrow NO_2 + O_2$	3.29×10^{-15}
(9) $NO_2 + h\nu \rightarrow NO + O$	1.63×10^{-3} s^{-1}
(10) $OH + O_3 \rightarrow HO_2 + O_2$	2.1×10^{-14}
(11) $HO_2 + NO \rightarrow OH + NO_2$	1.08×10^{-11}
(12) $O_3 + HO_2 \rightarrow OH + O_2 + O_2$	7.6×10^{-16}
(13) $NO_2 + NO_3 \rightarrow N_2O_5$	8.5×10^{-13}
(14) $N_2O_5 \rightarrow NO_2 + NO_3$	3.2×10^{-7} s^{-1}
(15) $N_2O_5 + h\nu \rightarrow NO_2 + NO_3$	2.76×10^{-6} s^{-1}
(16) $NO_2 + O_3 \rightarrow NO_3 + O_2$	1.5×10^{-18}
(17) $NO_3 + h\nu \rightarrow NO + O_2$ $\rightarrow NO_2 + O$	0.80×10^{-2} s^{-1} 1.81×10^{-2} s^{-1}
(18) $NO + NO_3 \rightarrow NO_2 + NO_2$	8.7×10^{-12}
(19) $OH + ClNO_3 \rightarrow HOCl + NO_3$	2.6×10^{-13}
(20) $ClO + HO_2 \rightarrow HOCl + O_2$	3.8×10^{-12}
(21) $HOCl + h\nu \rightarrow Cl + OH$	2.84×10^{-5} s^{-1}
(22) $HOCl + OH \rightarrow H_2O + ClO$	7.5×10^{-14}
(23) $ClO + O \rightarrow Cl + O_2$	4.2×10^{-11}
(24) $OH + CO(+O_2) \rightarrow CO_2 + HO_2$	1.88×10^{-13}
(25) $O(^1D) + H_2O \rightarrow OH + OH$	2.3×10^{-10}
(26) $O(^1D) + CH_4 \rightarrow OH + CH_3$	1.3×10^{-10}
(27) $HNO_3 + h\nu \rightarrow OH + NO_2$	4.92×10^{-9} s^{-1}
(28) $OH + HNO_3 \rightarrow H_2O + NO_3$	8.9×10^{-14}
(29) $OH + CH_4 \rightarrow H_2O + CH_3$	9.0×10^{-16}
(30) $Cl + HO_2 \rightarrow HCl + O_2$	4.5×10^{-11}
Temperature	217.15°K
Density	5.89×10^{18} cm^{-3}
O_3	3.32×10^{12} cm^{-3}
O	2.68×10^{4} cm^{-3}
$O(^1D)$	5.7×10^{-4} cm^{-3}
HNO_3	3.0×10^{-9} vol/vol
NO_t	0.5×10^{-9} vol/vol
H_2O	4.5×10^{-6} vol/vol
CH_4	1.0×10^{-6} vol/vol
CO	3.4×10^{-8} vol/vol

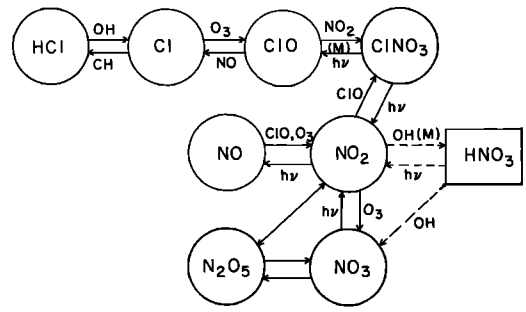

Fig. 2. Schematic diagram of chemical reactions affecting the Cl_x and NO_x species.

The curves showing the multiple solutions in Figures 1 and 7 may be readily calculated as follows. One must recognize that the steady state chemistry is no longer formally a function of Cl_x (i.e., single valued) but is still a function of the ClO density. Thus for a fixed value of ClO we solve for the densities of 10 species: Cl, HCl, HOCl, $ClNO_3$, NO, NO_2, NO_3, N_2O_5, OH, and HO_2. The required 10 nonlinear equations include a chemical steady state equation for nine of the above species (i.e., production = loss) plus an NO_t closure equation instead of NO_2 steady state. There is no Cl_x closure equation in this case, but ClO is specified over a range of values. Calculations with the more recent kinetics from *NASA/JPL* [1981] also included HNO_4 as a species in photochemical steady state.

Linear Stability Analysis

We need to analyze the stability of solutions to determine which of the possible steady states may occur in the atmosphere. The response of the system depends on the nature of the perturbation. It is necessary to specify whether the perturbation is infinitesimal or finite, constant or time dependent, homogeneous or spatially variable. We first consider the stability of arbitrary infinitesimal perturbations. The time evolution of the system is described by the following set of equations:

$$\partial n_i/\partial t = P_i(\mathbf{n}) - L_i(\mathbf{n}) = Q_i(\mathbf{n}) \tag{10}$$

where n_i is the concentration of species i and P_i and L_i are production and loss rates. Let the steady state concentrations $\mathbf{n}^0$ represent a solution to the set of equations $Q_i = 0$. If we consider small perturbations, then in the neighborhood of $\mathbf{n}^0$, stability of an infinitesimal perturbation depends on the eigenvalues of the Jacobian matrix J [*Carrier and Pearson*, 1968], given by

$$J_{ij} = \partial Q_i/\partial n_j \tag{11}$$

If the eigenvalues of the Jacobian matrix have negative real parts, the perturbation decays with time and the stationary state is stable. If at least one eigenvalue has a positive real part, the stationary state is unstable to infinitesimal perturbations.

Table 2 summarizes results for three steady states computed for 12 km, 60°N, winter, with $Cl_x = 7 \times 10^9$ and $NO_t = 3 \times 10^9$ cm^{-3}. Eigenvalues for the low and high ClO roots are negative. The middle root has one positive eigenvalue, and the corresponding steady state is unstable. The eigenvector associated with the positive eigenvalue of this root is shown in Table 3.

In summary, three distinct steady states are possible. Two are stable, one is unstable to infinitesimal perturbations. It remains to determine which if either of the stable states is preferred when the system is subjected to finite disturbances.

TABLE 2. Steady State Solutions for the Chemical Model in Table 1

Species	Number 1	Number 2	Number 3
ClO	1.17(6) cm^{-3}*	1.54(7)	1.12(9)
Cl	1.96(2) cm^{-3}	8.00(2)	2.88(3)
HCl	6.45(9) cm^{-3}	4.72(9)	6.00(8)
HOCl	5.72(4) cm^{-3}	3.13(6)	2.35(9)
$ClNO_3$	5.46(8) cm^{-3}	2.27(9)	2.99(9)
NO_2	1.85(9) cm^{-3}	6.12(8)	1.06(7)
NO	2.71(8) cm^{-3}	8.34(7)	5.88(5)
NO_3	3.28(5) cm^{-3}	1.10(5)	3.47(4)
N_2O_5	1.64(8) cm^{-3}	1.73(7)	1.01(5)
OH	7.12(3) cm^{-3}	3.97(4)	1.12(6)
HO_2	1.18(5) cm^{-3}	9.47(5)	1.33(7)
	Eigenvalues†		
	−2.8(+1) s^{-1}	−2.8(+1)	−2.8(+1)
	−1.2(−1) s^{-1}	−1.1(−1)	−1.0(−1)
	−3.0(−2) s^{-1}	−2.7(−2)	−3.2(−2)
	−1.3(−2) s^{-1}	−1.3(−2)	−2.6(−2)
	−3.1(−3) s^{-1}	−1.0(−3)	−5.0(−3)
	−9.5(−4) s^{-1}	−3.3(−4)	−1.8(−3)
	−2.8(−5) s^{-1}	−2.0(−5)	−3.1(−6)
	−3.8(−6) s^{-1}	−3.3(−6)	−1.3(−6)
	−2.4(−8) s^{-1}	+7.8(−8)	−4.9(−7)

$Cl_x = 7 \times 10^9$ cm^{-3} and $NO_t = 3 \times 10^9$ cm^{-3}.
* Read density as 1.17×10^6 cm^{-3}.
† Eigenvalues of the Jacobian matrix for each solution do not include the two degenerate zero eigenvalues resulting from the implied closure on Cl_x and NO_t. Calculations employed software from the Scientific Subroutine Package with 64-bit arithmetic.

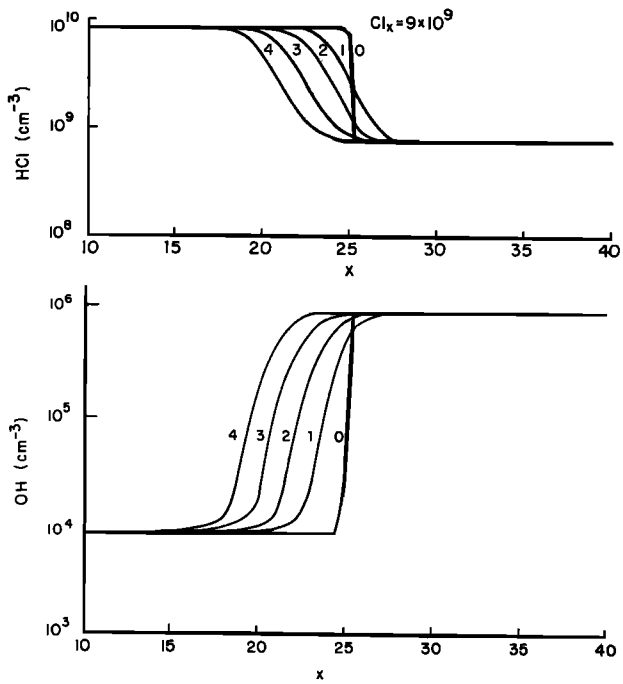

Fig. 3. Time-dependent evolution of the interface between two stable steady states as measured by the concentrations of HCl and OH. The system is one-dimensional, and the units on the x axis denote the actual resolution of the grid. The initial conditions (curve 0) comprise the low-ClO, high-NO_2 solution for $x < 25$ and the high-ClO, low-NO_2 solution for $x > 25$. Subsequent curves are labeled with time in units of 10^7 s. Total chlorine (Cl_x) is 9×10^9 cm^{-3}. The units of the x grid are 3000 $D^{1/2}$ cm.

PROPAGATION OF A FRONT

Consider a model in which semi-infinite volumes of the two steady states are put into contact. Perturbations arise from transport of species via diffusion or by turbulent mixing across the interface separating the two phases. If the two states are not equally stable, they may not coexist. The interface, after attaining its equilibrium shape, will move in time as the more stable state annihilates the less. This propagating front is called a soliton. *Ortoleva and Ross* [1975] discussed the theory of propagating fronts in simple chemical systems with multiple steady states. In systems not described by a potential, the relative stability of the two solutions may depend on the path connecting them, and the direction of motion of the soliton may be influenced by the shape of the interface [*Ortoleva and Ross*, 1975].

The length L and velocity v of the soliton are determined by a balance between diffusion and chemistry. When the interface achieves its steady state configuration, the time τ for diffusion across the interface (L^2/D) must equal the time required for the less stable solution to evolve chemically into the more stable state. The interface will propagate at a velocity given by

$$v = D/L = (D/\tau)^{1/2} \tag{12}$$

where D is the diffusion coefficient (cm^2 s^{-1}). The direction of propagation depends on values of the various constants, in this case temperature, insolation, Cl_x, NO_t, and other input parameters.

It is of particular interest to consider the variation in velocity of solitons corresponding to different concentrations of Cl_x. Figure 1 shows that multiple solutions occur at 12 km, 60°N winter, over a range of Cl_x from about 3×10^9 to 10×10^9 cm^{-3} for $NO_t = 3 \times 10^9$ cm^{-3}. Only one solution exists for Cl_x less than 3×10^9 cm^{-3}. By continuity, we might expect the low-ClO solution to be more stable as Cl_x increases into the regime of multiple solutions. Similarly, the high-ClO solution should be more stable near $Cl_x = 10 \times 10^9$. Both steady states should coexist, and the soliton velocity should vanish at an intermediate value of Cl_x.

The time dependent reaction-diffusion equations in one dimension may be written in the form

$$\partial n_i/\partial t = Q_i - D_i\, \partial^2 n_i/\partial x^2 \tag{13}$$

where D_i are transport coefficients. The chemical time scales associated with species i range over 9 orders of magnitude. We used a three-point spatial difference scheme with backward (implicit) differencing in time as discussed, for example, by *Acton* [1970, pp. 442–447; cf. *Logan et al.*, 1978].

TABLE 3. Eigenvector Associated With the Positive Eigenvalue $+7.8 \times 10^{-8}$ of the Middle Solution of Table 2

Species	Coefficient
ClO	+0.030
Cl	$+3.2 \times 10^{-7}$
HCl	−1.0
HOCl	+0.0096
$ClNO_3$	+0.96
NO_2	−0.75
NO	−0.12
NO_3	-1.4×10^{-4}
N_2O_5	−0.044
OH	$+6.0 \times 10^{-5}$
HO_2	$+1.7 \times 10^{-3}$

The sign (scaling) of the eigenvector is arbitrary; the present form points toward the high ClO, low NO_2 solution.

The equations were solved on a 50-point grid with uniform intervals Δx. The two stable steady states were separated initially by an interval containing the unstable solution. Boundaries were characterized by a condition of zero flux, with the interface kept well away from the boundaries. For most of the calculations presented here, we set $D = 1\ \text{cm}^2\ \text{s}^{-1}$ for all species and $\Delta x = 3000$ cm. For $D' \neq 1$, distances must be scaled by

$$\Delta x' = 3000(D')^{1/2}\ \text{cm} \tag{14}$$

Time scales are unaffected, and thus velocities will be proportional to $D^{1/2}$ [*Nitzan et al.*, 1974*a*].

Figure 3 illustrates the evolution of the interface for $Cl_x = 9 \times 10^9\ \text{cm}^{-3}$. Figure 3*a* shows the concentration of HCl, and Figure 3*b* shows the concentration of OH as a function of x, the distance along the grid. The curves are labeled by time in units of 10^7 s. The soliton attains its equilibrium shape in about 10^6 s, moving to the left with a velocity near $4.5 \times 10^{-4}\ (D^{1/2})$ cm s^{-1}. The high-ClO solution annihilates the low-ClO solution and may be considered therefore more stable. The soliton slows as Cl_x decreases until the velocity reaches zero at the point of coexistence of the two solutions. The soliton reverses direction for lower values of Cl_x as the low-ClO state becomes more stable. The behavior is illustrated in Figure 4, which shows the position of the interface as a function of time for four values of Cl_x. The soliton velocity decreases between $Cl_x = 9 \times 10^9$ cm^{-3} and $Cl_x = 5 \times 10^9\ \text{cm}^{-3}$. The direction of the soliton reverses at $Cl_x = 3.5 \times 10^9\ \text{cm}^{-3}$.

As the soliton velocity decreases, the effective width of the interface increases from about $5 \times 10^3\ (D^{1/2})$ cm for $Cl_x = 9 \times 10^9\ \text{cm}^{-3}$ to $1.5 \times 10^4\ (D^{1/2})$ cm for $CL_x = 3.5 \times 10^9\ \text{cm}^{-3}$. The time required for the interface to attain its equilibrium shape increases with diminishing velocity of the soliton. The chemical time constant associated with the soliton (12) is about 2×10^7 s and is presumably set by reaction of OH with HCl.

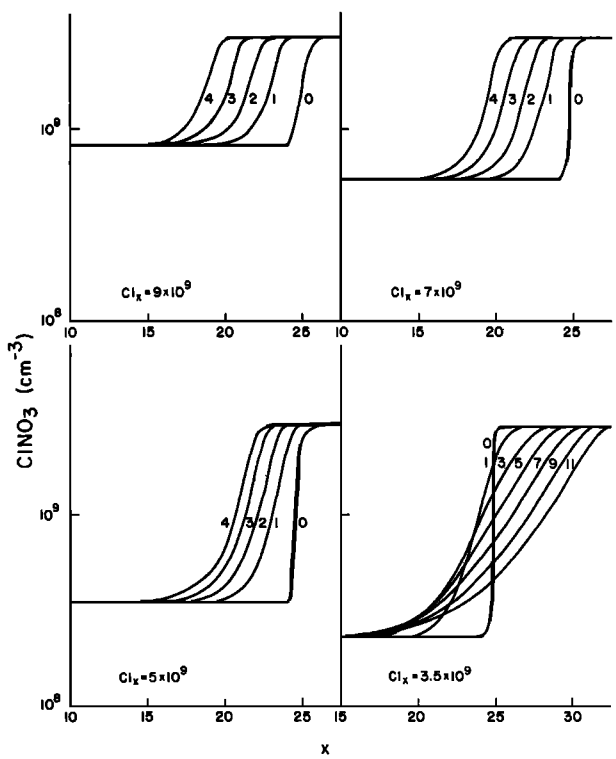

Fig. 4. Time-dependent evolution of the interface between two stable steady states, as measured by the concentration of $ClNO_3$ (see Figure 3). The behavior is shown for four values of Cl_x spanning the range of multiple solutions.

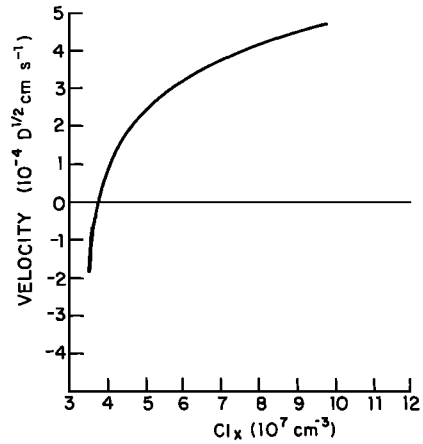

Fig. 5. The velocity of the interface (soliton) as a function of Cl_x.

Figure 5 shows the soliton velocity as a function of Cl_x. Coexistence occurs near $Cl_x = 4 \times 10^9\ \text{cm}^{-3}$. The exact location of coexistence is difficult to determine, since the integration times become long as the velocity approaches zero. The high-ClO, low-NO_2 solution appears more stable over almost the entire range of multiple solutions. The stability of the low-ClO solution is greater only in a limited region near $Cl_x = 3 \times 10^9\ \text{cm}^{-3}$.

STABILITY OF A FINITE PARCEL

A system initially in the less stable of the two possible steady states discussed above is not disturbed by infinitesimal perturbations. We may ask how large the perturbation must be to cause change. Consider a one-dimensional system characterized by the less stable state, to which we add an air parcel with composition described by the more stable solution. Figure 6*a*

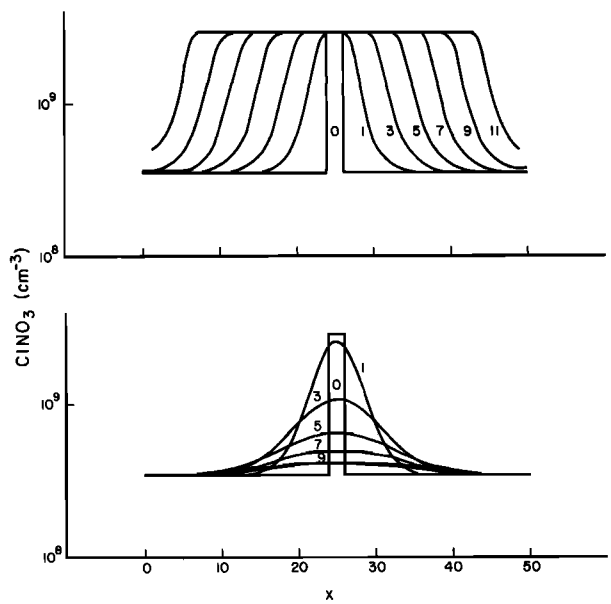

Fig. 6. Time-dependent behavior of a parcel of the high-ClO, low-NO_2 solution placed in the low-ClO, high-NO_2 solution. The system is one-dimensional, see Figure 3. In the top panel the grid scale is 1800 $D^{1/2}$ cm, and the pulse of width 3600 $D^{1/2}$ cm is observed to grow. The scale in the lower panel is 1500 $D^{1/2}$ cm, and the pulse of width 3000 $D^{1/2}$ cm disperses. Curves are labeled with elapsed time expressed in units of 10^7 s, and $Cl_x = 5 \times 10^9\ \text{cm}^{-3}$.

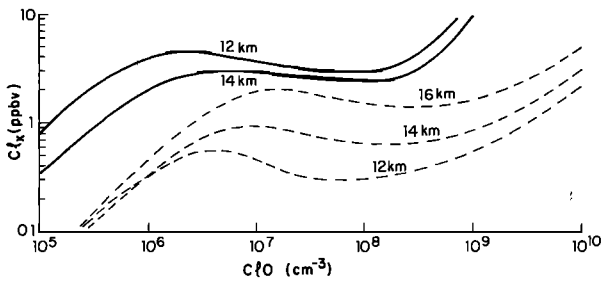

Fig. 7. Total chlorine (Cl_x) as a function of the concentration of ClO. The curves are labeled with altitudes for 60°N winter conditions. The dashed curves are from *Prather et al.* [1979] and correspond to a range in concentrations of NO_t and HNO_3 as described therein. The solid curves are based on more recent kinetic data [*NASA/JPL*, 1981] with $NO_t = 0.5$ ppbv and $HNO_3 = 3.0$ ppbv.

shows the evolution of the combined system for a pulse initially 3600 ($D^{1/2}$) cm wide. These calculations employed grid sizes which varied from $\Delta x = 1500$ cm to 1800 cm. As in the single interface problem, the more stable solution annihilates the less stable. The two interfaces move outward, increasing the size of the pulse until the entire volume is in the more stable configuration. If the initial pulse is small enough the behavior is different, as shown in Figure 6*b*. A pulse with initial width of 3000 ($D^{1/2}$) cm disappears and relaxes to the less stable state in about 10^8 s. For parcels smaller than some critical size, diffusion forces concentrations away from the more stable state before the parcel can grow, as discussed, for example, by *Schlogl* [1972], *Nitzan et al.* [1974*a*], and *Ortoleva and Ross* [1975]. The critical radius is near 3050 ($D^{1/2}$) cm for $Cl_x = 5 \times 10^9$ cm^{-3}. The phenomenon is analogous to that observed in the nucleation of droplets. There is a critical radius above which the embryonic droplet will grow, below which it dissipates.

Model Sensitivity and Diurnal Forcing

Sensitivity of results to details of the chemical model was tested by examining the regime of multiple solutions with the full photochemical model [*Logan et al.*, 1978] and with the more recent kinetic data of *NASA/JPL* [1981]. The family of multiple solutions was located for conditions discussed above. The new solutions are compared with the original calculations of *Prather et al.* [1979] in Figure 7. The solutions remain essentially unchanged despite significant changes in kinetic data. The domain of multiple solutions is observed to shift toward higher values of Cl_x, but the general behavior is similar.

We restricted our attention to systems in which insolation and concentrations of O and $O(^1D)$ were averaged over 24 hours. The energy flux from the sun is periodic, however, and many reactive species virtually disappear at night. We found two periodic solutions to the time-dependent kinetic equations with diurnal forcing. As shown in Table 4, the most significant difference between the diurnal and averaged solutions is the much greater importance of N_2O_5 in the diurnal case.

Conclusion

Prather et al. [1979] showed that the steady state equations describing NO_t and Cl_x at high latitudes in the winter stratosphere have multiple solutions. We showed here that two of the solutions, characterized by high and low ClO, are stable to infinitesimal perturbations while the third, an intermediate case, is unstable. We used the same chemical model as *Prather et al.* [1979] to allow comparison with the earlier work. Similar behavior is observed with reaction schemes favored in more recent stratospheric investigations. The earlier study used averaged values for insolation. Multiple steady states are found also when models allow for diurnal variation.

The high-ClO, low-NO_2 solution is more stable under most conditions. The low-ClO, high-NO_2 solution is favored only for a narrow range of NO_t near Cl_x. The sharp decline in stratospheric NO_2 between 40° and 50°N observed by *Noxon* [1975] in the winter of 1974–1975 could reflect the dominance of the high ClO, low NO_2 solution. *Prather et al.* [1979] showed that the possibility of multiple solutions first appears near 50°N and extends to higher latitude. In the presence of fluctuations, the atmosphere will be forced into this state, regardless of initial conditions. The transition may be abrupt, reflecting the discontinuous nature of multiple solutions.

Conversion of HCl to Cl, ClO, and $ClNO_3$ is limited by low concentrations of OH in the present model. The associated time constant is long, about 3×10^7 s, raising questions concerning the applicability of the model under realistic conditions. A more complete investigation will require simulation of both transport and chemistry during the transition from fall to winter. Time constants are relatively short in fall, less than 10^7 s, and the atmosphere should evolve rapidly toward the high-ClO, low-NO_2 state during this transition.

The present analysis constitutes a second step in a complete study of chemical bifurcations in the stratosphere. The bifurcation discussed here requires that Cl_x concentrations exceed NO_t, allowing titration of NO_t by ClO, resulting in large concentrations of $ClNO_3$. Since CFMs and CH_3CCl_3, the precursors of stratospheric chlorine, are increasing rapidly with time,

TABLE 4. Component Species of the Cl_x and NO_x Families for the Two Stable Solutions (60°N Winter at 12 km)

	Low ClO, High NO_2		High ClO, Low NO_2	
Species	Average	Diurnal (Noon)	Average	Diurnal (Noon)
ClO	0.0001 ppbv	0.0004 ppbv	0.04 ppbv	0.013 ppbv
HCl	3.42 ppbv	3.42 ppbv	2.97 ppbv	3.03 ppbv
$ClNO_3$	0.08 ppbv	0.08 ppbv	0.46 ppbv	0.44 ppbv
NO	0.07 ppbv	0.02 ppbv	0.001 ppbv	0.002 ppbv
NO_2	0.26 ppbv	0.12 ppbv	0.06 ppbv	0.006 ppbv
HNO_4	0.08 ppbv	0.08 ppbv	0.03 ppbv	0.05 ppbv
N_2O_5 (×2)	0.01 ppbv	0.20 ppbv	0.000 ppbv	0.001 ppbv
HNO_3 (fixed)	3.00 ppbv	3.00 ppbv	3.00 ppbv	3.00 ppbv
OH	6.1×10^3 cm^{-3}	1.8×10^4 cm^{-3}	4.8×10^4 cm^{-3}	5.8×10^4 cm^{-3}

Calculations here used kinetics from *NASA/JPL* [1981], not from Table 1.

abrupt changes in chemical regime may be expected to occur over a much larger region of the atmosphere in the future.

Acknowledgments. We would like to acknowledge support from National Aeronautics and Space Administration grants NSG-2031 and NSG-7176 and from National Science Foundation grant ATM79-13251. Jane L. Fox acknowledges support from the National Science Foundation post-doctoral fellowship program.

REFERENCES

Acton, F. S., *Numerical Methods That Work*, Harper and Row, New York, 1970.

Carrier, G. F., and C. E. Pearson, *Ordinary Differential Equations*, Blaisdell, Waltham, Mass., 1968.

Hahn, H. S., A. Nitzan, P. Ortoleva, and J. Ross, Threshold excitations, relaxation oscillations, and effect of noise in an enzyme reaction, *Proc. Nat. Acad. Sci.*, *71*, 4067–4071, 1974.

Logan, J. A., M. J. Prather, S. C. Wofsy, and M. B. McElroy, Atmospheric chemistry: Response to human influence, *Philos. Trans. R. Soc. London Ser. A*, *290*, 187–234, 1978.

National Aeronautics and Space Administration/Jet Propulsion Laboratory, Chemical Kinetic and Photochemical Data for Use in Stratospheric Modelling, *JPL Publ. 81-3*, Pasadena, Calif., 1981.

Nicolis, G., and I. Prigogine, *Self-Organization in Non-Equilibrium Systems*, Wiley-Interscience, New York, 1977.

Nitzan, A., and J. Ross, Oscillations, multiple steady states and instabilities in illuminated systems, *J. Chem. Phys.*, *59*, 241–250, 1973.

Nitzan, A., P. Ortoleva, and J. Ross, Nucleation in systems with multiple stationary states, *Faraday Symp. Chem. Soc.*, *9*, 241–253, 1974*a*.

Nitzan, A., P. Ortoleva, and J. Ross, Symmetry breaking unstabilities in illuminated systems, *J. Chem. Phys.*, *60*, 3134–3143, 1974*b*.

Nitzan, A., P. Ortoleva, J. Deutch, and J. Ross, Fluctuations and transitions at chemical instabilities: the analogy to phase transitions, *J. Chem. Phys.*, *61*, 1056–1074, 1974*c*.

Noxon, J. F., Nitrogen dioxide in the stratosphere and troposphere measured by ground-based absorption spectroscopy, *Science*, *189*, 547–549, 1975.

Ortoleva, P. J., and J. Ross, Instabilities in coupled chemical reactions with pressure-dependent rate coefficients, *J. Chem. Phys.*, *55*, 4378–4390, 1971.

Ortoleva, P., and J. Ross, Theory of propagation of discontinuities in kinetic systems with multiple time scales: Fronts, front multiplicity, and pulses, *J. Chem. Phys.*, *63*, 3398–3408, 1975.

Prather, M. J., M. B. McElroy, S. C. Wofsy, and J. A. Logan, Stratospheric chemistry: Multiple solutions, *Geophys. Res. Lett.*, *6*, 163–164, 1979.

Prigogine, I., and G. Nicolis, On symmetry-breaking instabilities in dissipative systems, *J. Chem. Phys.*, *46*, 3542–3550, 1967.

Schlogl, F., Chemical reaction models for non-equilibrium phase transitions, *Z. Phys.*, *253*, 147–161, 1972.

Turing, A. M., The chemical basis of morphogenesis, *Philos. Trans. R. Soc. London Ser. B*, *237*, 37–72, 1952.

World Meterological Organization, The Stratosphere 1981: Theory and Measurements, *Global Ozone Res. Monit. Proj. Rep. 11*, edited by R. D. Hudson et al., Geneva, Switz., 1981.

(Received March 15, 1982;
revised September 14, 1982;
accepted September 15, 1982.)